MAGNETIC GUIDING OF A MOVING FERROMAGNETIC SPHERE

Darryl S. Jessie[1, *] and Michael P. Bradley[2]

[1]Qualcomm Inc., San Diego, CA 92121, USA

[2]Department of Physics & Engineering Physics, University of Saskatchewan, Saskatoon S7N 5A2, Canada

Abstract—This article describes a method of guiding a moving ferromagnetic sphere. By using a magnetic field, it is possible to confine a moving object such as a steel sphere to motion along a curve. We have designed and built a device that uses the magnetic field in the gap of a steel tube to trap and guide a steel sphere along a circular path solely by a magnetic restoring force. A simple relationship between tangential velocity and magnetic field strength in the gap is developed. Excellent correlation between analytic, simulated, and measured results are shown.

1. INTRODUCTION

A force that confines an object to a specified path has been the object of public and scientific interest for many years, and much of this effort has been in the field of magnetic levitation [1–3]. Much effort over a long period of time has been applied to moving objects with magnetic forces [4, 5], with application in the fields of mass drivers and electromagnetic braking [6–8]. Moving an object with magnetic forces while mechanically confined to a curve has been applied to magnetically levitated trains and magnetic actuators [9]. Di Puccio et al. have done some interesting work with magnetic bearings that includes off-axis development of force equations [10], which is related to the work we will present in this paper. However, we have developed a unique expression concerning the confining of a non-atomic scale projectile to a curve with magnetic forces alone.

We have developed a method to guide a steel sphere such as a ball-bearing along a curved path. One can view the sphere as suspended along an arc in the plane of motion since a balance is obtained between the centripetal and magnetic forces. Figure 1 illustrates the concept of what we are trying to achieve; a steel sphere is injected into a steel pipe bent into a half-toroid. The tube has a slot cut on the outer edge, and current-carrying conductors on the inner edge. This creates a magnetic field in the slot. If a steel sphere is injected in the slot, it will either leave the confinement of the slot and exit the tube, or continue along the slot and exit the tube on the opposite side.
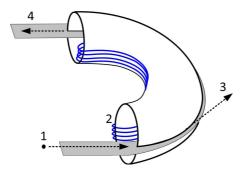

Figure 1. A conceptual method to restrain a steel sphere along curved path with magnetic forces: a steel sphere is injected (1) into a curved steel tube with a slot cut on the outer edge and a coil wrapped along its interior edge (2), the sphere will either exit the slot if travelling too fast (3) or be confined to the slot and exit out the other side (4).

This paper contains a unique development of the force equations from first principles, and in conjunction with two-dimensional (2D) Finite-Element Method (FEM) simulations and experimental results, a simple expression is derived which relates the magnetic field in the gap acting on the sphere to its tangential velocity.

2. THEORETICAL DEVELOPMENT

A cross-section of the tube in Figure 1 is shown in Figure 2. This is simply the C-shaped core familiar to students of magnetic circuit theory. The windings around the core carry current, and the core is made from a material such as mild steel with relative permeability μ_r much greater than 1.

There will be a force drawing the steel sphere into the centre of the gap, since there exists a magnetic field gradient in every direction away from this center-point. For our problem, the magnetic force $\vec{F}_m$
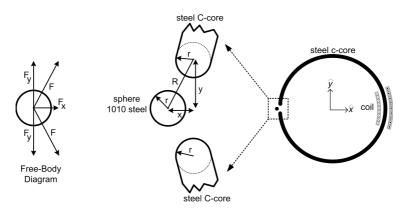
Figure 2. An enlarged cross-section of the gap in a C-core with a current carrying coil providing a magnetic field in the gap. The cross-section of the C-core ends and sphere resemble three magnetic conductors in free space. On the far left is the free-body diagram of the magnetic forces on the sphere.

can be understood as the gradient of the magnetic energy density U_m multiplied by the volume V the magnetic field occupies:

$$\vec{F}_m = -\vec{\nabla} U_m V \tag{1}$$

$$F_m(x, y) = -\frac{1}{2\mu_0} \frac{dB^2(x, y)}{dx} V = -\frac{B(x, y)}{\mu_0} \frac{dB(x, y)}{dx} V \tag{2}$$

where B is the magnetic field strength, and an isotropic medium and motion in the x-direction is assumed. If the sphere is free to move in any direction, slight changes in its vertical position with respect to the poles will cause the sphere to become stuck on one of the poles. In other words, the y-component of the force will become imbalanced and the sphere will move toward the pole. For our case, we will purposely design a slight offset in the y position of the sphere to insure the sphere will stay near the middle of the gap in the y-dimension. We can do this by utilzing the intrinsic weight of the sphere to hold it down along a non-magnetic guide, and also implementing 0.15 mm offset to insure the vertical component of magnetic force is slightly downward. Then with these precautions in place, we can focus on the magnetic force require to suspend the sphere in the x-direction as it travels around the curve.

In a magnetic circuit, the majority of the magnetic energy is concentrated in the air gap, and it is this change in air gap that occurs if the ferromagnetic object is free to move. In a general sense, an infinitesimal displacement of the object will cause the gap volume to change, which is the surface area A times air gap length. Equation (2)

then becomes:

$$F_m = -\frac{1}{2\mu_0}\frac{dB^2}{dL_g}AdL_g = -\frac{B^2 A}{2\mu_0} \tag{3}$$

which is the familiar magnetic force equation between two magnetized bodies.

In order for the sphere to travel on a curve with radius of curvature a, the magnetic field may provide enough force necessary to allow the sphere to travel in a curved path. A simple relationship can then be developed between the magnetic and centripetal forces F_c:

$$F_m = F_c = \frac{mv_t^2}{a} \tag{4}$$

$$v_t = \sqrt{\frac{F_m a}{m}} \tag{5}$$

where m is the mass of the object and v_t is the tangential velocity of the sphere. By substituting into Equation (5) an explicit expression for the magnetic force, which will depend on the geometry and magnetic field strength in the gap, we can obtain an expression for the upper limit of ferromagnetic sphere velocities that will be confined.

2.1. Analytic Derivation of Magnetic Force

With the advent of powerful 2D and 3D electromagnetic simulation tools, complicated geometries such as this one can be solve numerically. However, by attempting to solve the problem analytically, we believe further insights will be found and scalings will be revealed that are hard to see by relying solely on simulated results.

In order to develop the magnetic force equation, we will simplify the C-core tips in Figure 2 into cross-sections of long parallel cylinders. The magnetic force on the cross-section of the sphere in the x- and y- directions is then the vector sum of the components due to the lower and upper core ends, i.e., the core ends are assumed to be 2D cross-sections of cylinders with magnetic surface charge and floating in free space. The magnetic circuit is then the C-core plus sphere (both of the same ferromagnetic material) in series with two air gaps.

The magnetic force is proportional to the gradient of the permeance ($\mathcal{P}$) multiplied by the square of the "magnetomotive force" (essentially, the total applied Amp · turn product). The magnetomotive force can be written in simplified form:

$$NI = \frac{\phi}{\mathcal{P}} \tag{6}$$

If we can find the magnetic flux ϕ of the circuit, it can then be written in a general sense:

$$F_m = \frac{1}{2}\left(\frac{\phi}{\mathcal{P}}\right)^2 \frac{d\mathcal{P}}{dR} = \frac{B^2 A^2}{2\mathcal{P}^2}\frac{d\mathcal{P}}{dR} \tag{7}$$

where R is the distance between centres as in Figure 2. In our configuration, the sphere will have a non-magnetic standoff to ensure the sphere is near the $y=0$ plane, thus removing the vertical degree of freedom of its motion.

The value of ϕ can be estimated by solving the magnetic circuit equation:

$$NI = (\mathcal{R}_{core} + 2\mathcal{R}_{gap} + \mathcal{R}_{sphere})\,\phi \tag{8}$$

$$NI = \left(\frac{L_c}{\mu_r\mu_o W} + \frac{2L_g}{\mu_o W} + \frac{L_s}{\mu_r\mu_o W}\right)\phi \tag{9}$$

where reluctance $\mathcal{R}$ is the inverse of permeance, the flux path length for each element is L, and flux path width W is simplified to the width of the core. A classic problem with magnetic circuits is what to choose for the relative permeability μ_r for a non-linear material such as mild steel, something we will return to later.

Once we have an estimate for magnetic flux, we can leverage the analysis described by Roters [11] and utilize the fact that the permeance from the C-core ends to the sphere can be derived from potential theory, which is essentially the solution to Laplace's equation. For our 2D parallel cylinder configuration it is equal to:

$$\mathcal{P} = \frac{\mu_o\pi}{\ln\left(\frac{R}{2r} + \sqrt{\left(\frac{R}{2r}\right)^2 - 1}\right)} \qquad [p.u.l.] \tag{10}$$

where μ_o is the magnetic permeability of free space. The derivative of the permeance with respect to spacing R is then:

$$\frac{d\mathcal{P}}{dR} = \frac{-\mu_o\pi}{2r\left(\sqrt{\left(\frac{R}{2r}\right)^2 - 1}\right)\left[\ln\left(\frac{R}{2r} + \sqrt{\left(\frac{R}{2r}\right)^2 - 1}\right)\right]^2} \tag{11}$$

Substituting Equations (11) and (10) into (7), the magnetic force per unit length is then obtained:

$$F_m = \frac{\phi^2}{4\pi r\mu_o\sqrt{\left(\frac{R}{2r}\right)^2 - 1}} \tag{12}$$

We can then take the x-component of the force and multiply by two since there are two 2D cylinders acting on the sphere. By placing

$\phi = BA$ into Equation (12) and substituting into Equation (5), we can obtain an expression for tangential velocity in terms of B:

$$v_t = \sqrt{\frac{B^2 A^2 a}{4\pi r m \mu_o \sqrt{\left(\frac{R}{2r}\right)^2 - 1}}} \qquad (13)$$

Since all terms except B^2 are constant for a given geometry and material, we can write:

$$v_t = \sqrt{\text{constant} * B^2} \qquad (14)$$
$$v_t = k * B \qquad (15)$$

where k is a constant that depends on geometry and mass of the object. This elegant result states that the maximum tangential velocity of the sphere traveling around a curve is linearly related to the magnetic field strength acting on the sphere.

2.2. Simulation Method to Obtain Magnetic Force

We would like to validate the accuracy of our magnetic force Equation (12), and for that we turn to a two-dimensional magnetic field solver such as Ansoft 2D Extractor — an excellent tool for obtaining the magnetic field strength in a 2D environment. In fact, Ansoft-2D will directly provide the per unit length (p.u.l) force on an object as part of the solution. It does this by calculating on the surface of an object the magnetic field strength and gradient of the meshed magnetic field values and applying Equation (2).

Our first simulation had a 6.35 mm (1/4") diameter cross-section of a ball-bearing placed between C-core ends with a center-to-center vertical separation of 18.0 mm (11.6 mm between core ends) and offset 4.7 mm from the horizontal center of the C-core ends. For this case, 260 Amp-turns constitute the coil magnetomotive force. The simulation results are shown in Figure 3, which is a cross-section of the B-field strength in the plane of the gap.

The magnetic force per unit length obtained from the simulation was 1.44 N in the positive x-direction (to the right in the figure). To solve this analytically, we used Equation (9) to find the magnetic flux in the circuit, then applied Equation (12) to get the force. As mentioned before, the relative permeability of mild steel is non-linear. Ansoft 2D supplies material properties in their materials database, and for 1010 steel, the μ_r changes from 0 at no excitation, to 600 at 0.21 T. The simulation indicates that at the excitation coil, the magnetic field strength in the core is around 0.15 T, while at the core tips it is near 0.05 T (due to leakage to free space). A reasonable assumption for the
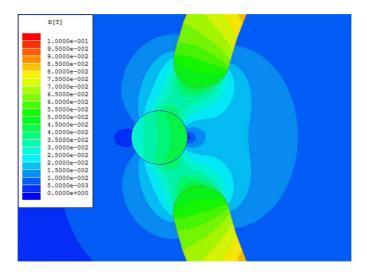
Figure 3. Simulated magnetic fields for 1/4" diameter marble and rounded C-core ends.

μ_r in the steel is around 100. In fact, if we complete the calculation of magnetic force using μ_r of 70, the calculated magnetic force equals 1.43 N, which matches the simulation results.

This procedure highlights both the strength and weakness of the analytic approach to a geometry such as ours. The great strength is we can see the factors that affect the magnetic force on the sphere, which is important for magnetic circuit design. The weakness of the method is we need to obtain an accurate value for one of the magnetic parameters (B-field, ϕ, or μ_r) by some other method for an accurate calculation of force.

For comparison, we also ran simulations with the core ends flattened in the cross-section of Figure 3. Flattening the core ends will also make it easier to construct when manufacturing the test apparatus. Figure 4 shows the simulated B-field of the flattened pole face C-core. This provided a larger gradient and greater magnetic field strength on the surface of the sphere, thus increasing the magnetic force retaining the sphere along the guide. We used a Gaussmeter to measure the field in the gap without a sphere involved for the case of 400 Amp-turns. Simulated value in the middle of the gap was 0.0378 T, and the measurement provided approximately 0.039 T, which is good agreement and provide more confidence that the field values from simulations with a sphere involved are accurate. One can see in Figure 4 the peak magnetic field on the surface of the sphere is now 0.064 T, compared to 0.045 T in Figure 3.
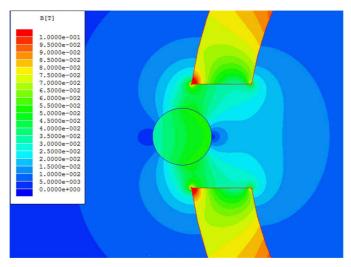
Figure 4. Simulation of force for a flattened C-core ends. The sphere is close to where the horizontal peak force is acting on it as it moves from left to right.

3. EXPERIMENTAL RESULTS

For this paper, we conducted two experiments. The first measured the magnetic force acting on a sphere in the gap of a C-core as the sphere is pulled out of the gap, and the second determined the relationship between centripetal and magnetic forces in the C-core gap. The cross-section used in these experiments is given in Figure 5.

A simple method to measure the peak force on the sphere as it moves laterally across the gap is to glue a thread between it and a force meter lever. The sphere is placed at the center of the gap and current is then applied to the coil. The force meter is then dragged away from the slot and the peak magnetic force is recorded on the display.
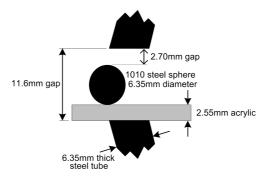

Figure 5. Flattened core end simulation and experimental setup.

In our setup, we designed a slight offset for the sphere in the vertical direction to create a small downward net magnetic force, which, in addition to its weight, helps reduce any bounce as the projectile leaves the ramp and enters the tube.

The measured peak magnetic force as the sphere is translated in Figure 5 is recorded in Table 1. Table 1 also includes the peak magnetic force from 2D simulations. In order to obtain the force acting on a three dimensional sphere from 2D simulations, we multiply the 2D results by the characteristic dimension of the sphere (the diameter of 0.00635 meters). Good agreement can be seen between measured and 2D simulated results multiplied by the correction factor. Note we have not corrected for thread weight or sliding friction, both of which are regarded as negligible.

Table 1. Peak force measured and simulated for 6.35 mm steel sphere.

Amp-Turns (A)	Measured (N)	2D Simulated (N)	2D Simulated w/Correction (N)
400	0.0294	4.94	0.0313
600	0.0736	11.48	0.0729
784	0.108	20.18	0.128

So far, we have only worked with low magnetic field values, to insure we are in a linear region of the BH curve in order to validate Equation (12). But what happens to the magnetic field in the gap and the force on the sphere as the Amp-Turns are increased? At some point, the permeability of the C-core steel becomes saturated and significant leakage flux bypasses the gap. This will have the effect of limiting the magnetic flux acting on the sphere and the force on the sphere will not change no matter what the Amp-Turn value. Table 2 contains simulated 2D data that shows for low values of magnetomotive force, there is a square relationship between Amp-Turns and force on the sphere, just as Equation (12) implies, meaning, for every doubling in Amp-Turns, the B-field doubles and force quadruples. However, for large Amp-turn values, the B-field and force saturate.

In the next phase of our experimentation, we have corroborated Equation (15) with experimental data by using a pipe section known in industry as a "180°-Return", as shown in Figure 6. Although the actual magnetic permeability of this mild steel was not known, using the values for 1010 steel provided good results in measurements and

Table 2. Force and magnetic field as a function of Amp-turns.

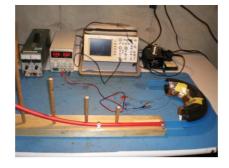| Amp-Turns (A)	B (T)	2D Simulated (N)	Square Dependency (Equation (12)) (N)
256	0.052	1.98	1.98
512	0.107	8.24	7.92
1280	0.275	53.7	49.5
2560	0.471	158	198
5120	0.556	221	792
25600	0.684	332	19800

Figure 6. Experimental setup. The marble ramp is the red tube, the black pipe on the right is the curved core, the blue acrylic guide insures the marble is near the center of the gap. If the marble is confined, it will exit the pipe section near the oscilloscope.

simulations. The radius of curvature to the outside edge of the pipe is approximately 168 mm (6-5/8").

A steel ball-bearing is released down the ramp (red) and it enters the 180°-Return gap (black tube). The sphere is offset in the gap by the acrylic guide (blue). By adjusting the amount of current in the coil and/or the release height of the marble so that it (just) exits from the arc, a relationship of maximum marble entry speed versus gap magnetic strength can be obtained. The injection velocity of the marble was calculated from $v = \sqrt{2gh}$, where g is the acceleration due to gravity $(9.81\,\mathrm{m/s^2})$ and h is the fall height in meters. In reality, if one includes the rotational energy gained, it will lower the translational velocity calculation by 15%. However, since the sphere is entering a region of B-field gradient as it exits the ramp, the projectile will
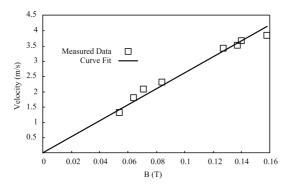
Figure 7. Injection velocity versus simulated peak magnetic field strength on surface of the sphere. The curve fit to measured data is $v\,[\mathrm{m/s}] = 26.6B\,[\mathrm{T}]$.

speed up slightly, and this partially makes up for the rotational energy not accounted for. The net effect is calculating the entry velocity by neglecting rotational energy provided good agreement.

The results of our experiment are shown in Figure 7. For guided motion, we obtained a linear relationship between injection velocity and magnetic field strength, as predicted.

The reader should note we did not correct for systematic velocity errors such as air or eddy current drag as the sphere travels around the curve. Recent papers regarding magnets moving near conductors indicate that at such low velocities, the eddy current drag will not play a significant role in slowing the projectile [12–14]. However, since there are losses, we have found if the sphere stays confined in the first 45 degrees of the 180 degree arc, it will stay confined the rest of the way around.

4. CONCLUSION

This paper describes the governing equations of a ferromagnetic sphere confined by a magnetic field and traveling on a curve. We have obtained excellent correlation between the developed theory, simulation, and experimental results. These results can be used for applications where ferromagnetic objects are required to move along non-linear trajectories, such as with directed energy and mass launcher applications. In addition, since many aspects of physics and engineering are developed in the paper (rotational motion and energy, magnetic forces, and magnetic circuits to name a few), the device would make an excellent classroom demonstration or lab experiment.

REFERENCES

1. Livingston, J. D., *Rising Force*, Harvard University Press, Inc., Cambridge, Mass., 2011.

2. Jayawant, B. V., *Electromagnetic Levitation and Suspension Techniques*, Edward Arnold (Publishers) Ltd., London, 1981.

3. Di Puccio, F., A. Musolino, R. Rizzo, and E. Tripodi, "A self-controlled maglev system," *Progress In Electromagnetics Research M*, Vol. 26, 187–203, 2012.

4. Hesmondhalgh, D. E. and D. Tipping, "Translational forces on discrete metallic objects in travelling magnetic fields," *IEE Proceedings*, Vol. 128, Part B, No. 3, 137–148, May 1981.

5. Thome, R. J., "Interaction of a traveling magnetic field with rigid conducting spheres or cylinders," *Proceedings of the IEEE*, Vol. 55, No. 12, 2116–2122, Dec. 1967.

6. Starr, S. O., R. C. Youngquist, and R. B. Cox, "The low voltage 'railgun'," *Am. J. Phys.*, Vol. 81, No. 1, 38–43, Jan. 2013.

7. Kaye, R. J., "Operational requirements and issues for coilgun electromagnetic launchers," *IEEE Transactions on Magnetics*, Vol. 41, No. 1, 194–199, Jan. 2005.

8. Pellicer-Porres, J., R. Lacomba-Perales, J. Ruiz-Fuertes, D. Martínez-García, and M. V. Andrés, "Force characterization of eddy currents," *Am. J. Phys.*, Vol. 74, No. 4, 267–271, Apr. 2006.

9. Urban, C., R. Gunther, T. Nagel, R. Richter, and R. Witt, "Development of a bendable permanent-magnet tubular linear motor," *IEEE Transactions on Magnetics*, Vol. 48, No. 8, 2367–2373, Aug. 2012.

10. Di Puccio, F., R. Bassani, E. Ciulli, A. Musolino, and R. Rizzo, "Permanent magnet bearings: Analysis of plane and axisymmetric V-shaped element design," *Progress In Electromagnetics Research M*, Vol. 26, 205–223, 2012.

11. Roters, H. C., *Electromagnetic Devices*, John Wiley & Sons, Inc., New York, 1941.

12. Tomasela, F. G. and M. C. Marconi, "Rolling magnets down a conductive hill: Revisiting a classic demonstration of the effects of eddy currents," *Am. J. Phys.*, Vol. 80, No. 9, 800–803, Sep. 2012.

13. Thompson, M. T., "Eddy current magnetic levitation," *IEEE Potentials*, Vol. 19, No. 1, 40–44, Feb./Mar. 2000.

14. Donoso, G., C. L. Ladera, and P. Martín, "Damped fall of magnets inside a conducting pipe," *Am. J. Phys.*, Vol. 79, No. 2, 193–200, Feb. 2011.